14 th Australasian Fluid Mechanics Conference
Adelaide University, Adelaide, Australia
10-14 December 2001

Modelling Of Fluid Flow In A 3-Axial Groove Water Bearing Using Computational Fluid Dynamics

R.Pai, D.J.Hargreaves and R. Brown

Tribology Research Concentration
Queensland University of Technology, Brisbane, Queensland, 4001, AUSTRALIA.

Abstract
This paper details a Computational Fluid Dynamics approach to model fluid flow in a journal bearing with three equi-spaced axial grooves and supplied with water from one end of the bearing. In the clearance space of the bearing, water is subjected to both velocity and pressure induced flow. A dedicated Computational Fluid Dynamics software has been used to model the fluid flow phenomenon. Results are presented for the circumferential and axial pressure distribution in the bearing clearance for different loads, speeds and supply pressures. Results are compared with experimentally measured pressure distributions.

Introduction
The research pertains to an electrical power generation authority considering the use of water lubricated bearings in circulating water pumps to be located in a river. Water lubricated bearings would represent an environmentally acceptable option. The use of oil lubricated bearings would lead to pollution of the river in case of a mechanical component malfunction. Due to tighter pollution regulation, water lubricated applications are expected to continue to grow. Hence, bearings must be able to operate hydrodynamically with very low viscosity fluids and are expected to survive in long term operation. To meet the trend toward using the process fluid, in this case water as the lubricant, a significant amount of theoretical and experimental development will be required.

Shelly and Ettles [6] analysed the performance of journal bearings with oil grooves that were positioned at the maximum pressure location. They discovered that positioning the grooves at the maximum pressure location will cause 30 to 70 percent reduction in the load capacity of the bearing. This results in the lowering of the film thickness between journal and bearing which could lead to journal bearing contact and hence increased wear [4].

Therefore, the provision of grooves should not be in the load carrying area and should be as close to the maximum film thickness which would least interfere with the hydrodynamic performance of the bearing. This would provide maximum performance [8]. In order to provide increased lubricant flow for better cooling and to reduce the shear force in certain parts of the journal bearing, it is sometimes necessary to extend the grooves through the load carrying area [3]. Thus it is important to note that improving one aspect of the bearing performance may have deleterious effects on other operating parameters. Therefore a complete bearing design must examine all aspects of the bearing performance.

The objectives of this study were to:

1. undertake an investigation into using computational fluid dynamics (CFD) approach to predict the pressure in the lubricant.
2. measure the pressure in the lubricant (water) film in the journal bearing operating with various conditions, in particular with 3-axial grooves equi-spaced around the bearing and with combined Couette flow and an orthogonal Poiseuille flow.

Modelling the water bearing

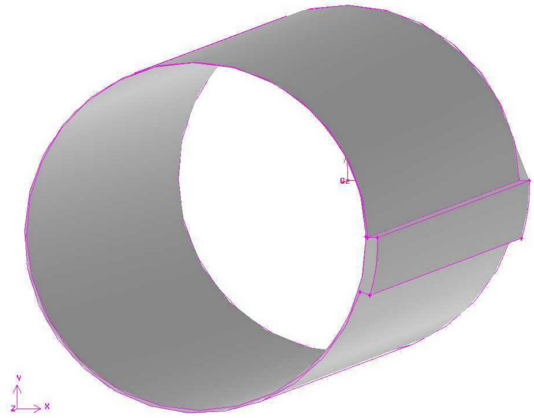

Figure 1. Model of the clearance volume showing one axial groove.

From the results of ESDU [1,2] computations the eccentricity ratio and attitude angle were available for each load and speed at which the bearing was run. These were used to model the clearance volume of the 3-axial groove bearing (figure 1).

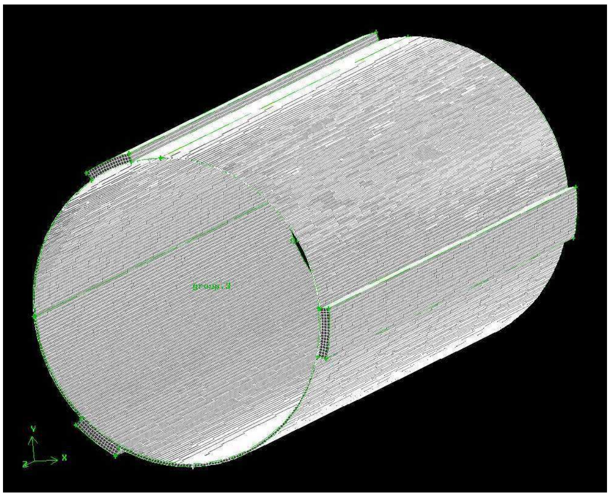

Figure 2. Meshed clearance volume with the 3-axial grooves.

Grid details
Figure 2 shows an unstructured mesh of the clearance volume.

Number of nodes in the meshed clearance volume=1,58,790
Number of mesh elements (hexahedral) = 92,800
Minimum skewness = 0.6

CFD analysis

A software package FLUENT 5.0 was used to predict the pressure distributions in the bearing. The CFD software is based on the four fundamental equations of fluid mechanics including turbulent and compressible flow. The computational domain is discretised into control volumes and the equations solved for pressure and velocity. Some difficulty was encountered on setting the pressure boundary conditions, in defining the mesh (because of the aspect ratio in lubrication problems, that is long thin volumes over which the equations need to be solved) and the solution of the system of equations.

Boundary conditions

The inlet to the bearing is at the rear in figure 2. and was set as type- 'pressure inlet' with the supply pressure 50 kPa, normal to the boundary.

The outlet of the bearing is at the front in Figure 2. and was set as type- 'pressure inlet' with the outlet pressure 42 kPa, normal to the boundary.

The bearing shell was modelled as a 'moving wall' with absolute motion of 0 rad/sec. The rotational axis origin was set at X=0, Y=0,Z=0 and direction of the axis was set as X=0, Y=0, Z= -1.

The journal was modelled as a 'moving wall' with a motion relative to the adjacent cell zone at an angular speed of 108.91 rad/sec (this angular speed is attained in steps as described below). The rotational axis origin for the journal was set at the eccentricity, which is X=0.0957 mm, Y=0.414 mm, Z=0 for a load of 3971.1 N and speed of 1000 rpm. The rotation axis direction was set as X=0, Y=0, Z=-1.

The water in the clearance volume was modelled as type- 'fluid', with rotation axis origin and direction same as that of the journal above. The rotational velocity was set at 108.91 rad/sec in the same manner as that for the journal. The translational velocity in all three coordinate directions was set equal to zero.

The segregated solver was used for the solution and the flow was assumed to be laminar and steady. Under-relaxation factors were required for both pressure and velocity equations. It was also found that the solution was frequently sensitive to these factors, so that the absolute values predicted by the software sometimes varied depending on the discretisation chosen for pressure, momentum and pressure-velocity coupling. The under-relaxation factors used for pressure, momentum, density and body forces are 0.3, 0.01,1 and 0.01 respectively for the solution. The discretisation used is 'presto' for pressure, 'quick' for momentum and 'simple' for the P-V coupling.

An interesting feature of the solution technique is that the angular velocity of the journal surface is varied in steps. The converged solution of the first step is used as the start point for the next step. The step size of the angular velocity is determined by halving the full angular velocity, which is again halved and so on. The halving process is stopped if it is determined that there are sufficient number of steps. If the step size is too small it may lead to unnecessary computations. It is necessary to arrive at a solution by varying the angular velocity in steps because of the curvature of the bearing surfaces. The solution is converged if the normalised residuals are of the order of $1x10^{-3}$. There was a difference in the predicted pressure contours and the experimentally measured contours. Figures 3 and 4 show the predicted pressure contours for two different loads at the same speed and supply pressure. Predicted axial pressure variations along a groove (figure 6) agreed with experimental trends from a qualitative perspective (figure 7). From a quantitative perspective there is a difference between the predicted and measured pressures.

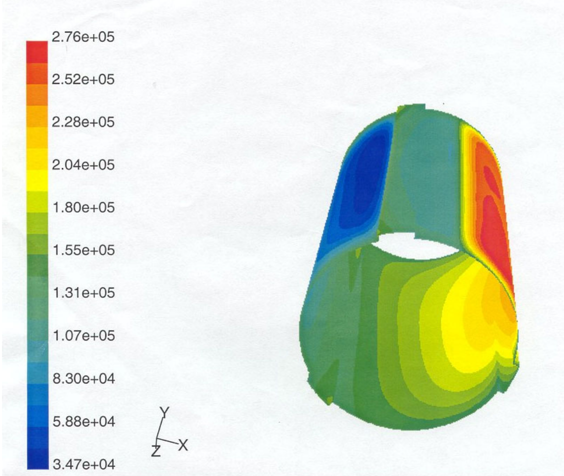

Figure 3. Pressure contours from FLUENT 5.O for 1000 rpm, 50 kPa 2976.35 N , 3mm, 36 degree groove (Pressure in Pascals).

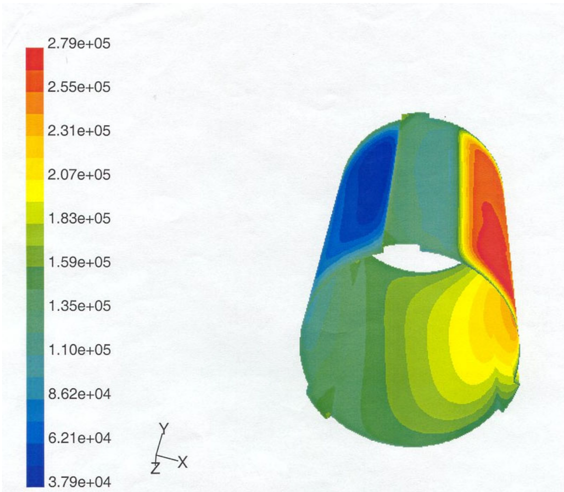

Figure 4. Pressure contours from FLUENT 5.0 for 1000 rpm, 50 kPa 3971.09 N, 3mm, 36 degree groove (Pressure in Pascals).

Experimental details

A bearing test rig shown schematically in figure 5 and described in [7], was developed to evaluate the non-metallic journal bearing performance when lubricated by water. The rig is configured to test bearings with 100mm bore diameter and length of 200mm at speeds up to 1500rpm and loads up to 9810 N. The bearing test rig was designed and built to provide reliable measurements for journal bearings with any number of grooves which extend from one end to the other end. For all tests reported here, the bearing material was an elastomeric material made from thermosetting resins which are three-dimensional cross-linked condensation polymers.

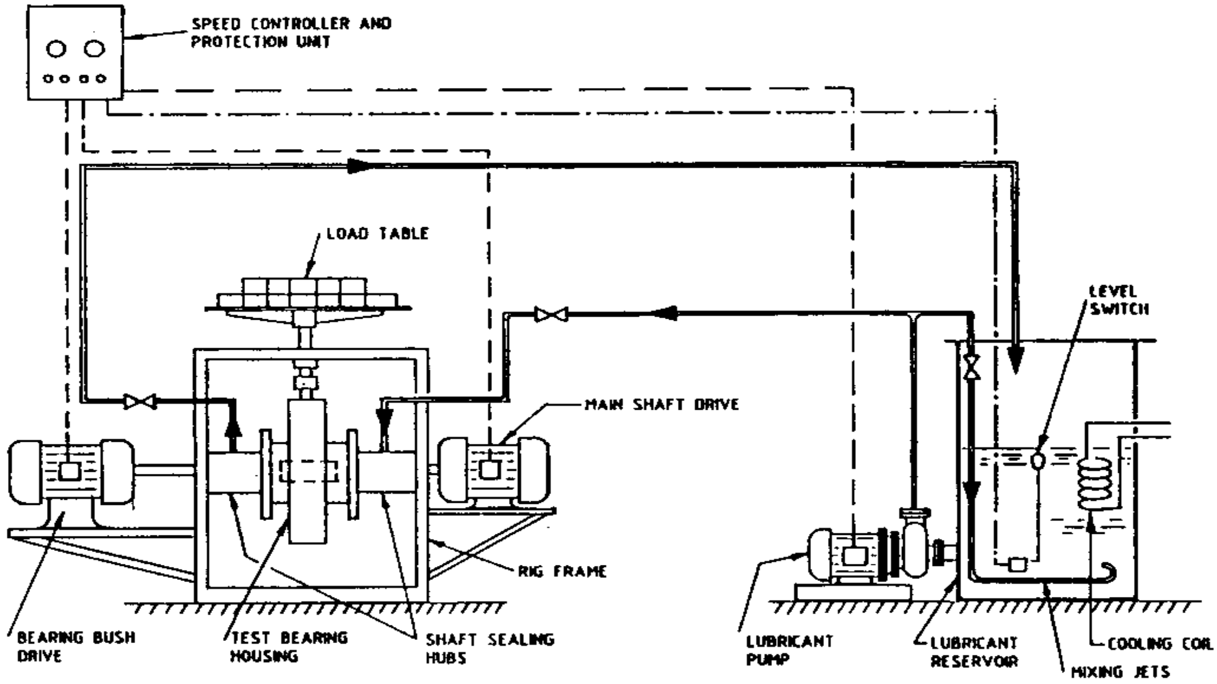

Figure 5. General arrangement of the bearing test rig.

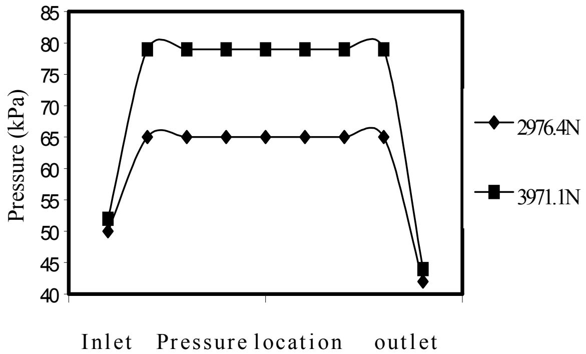

Figure 6. Axial pressure distribution from FLUENT 5.0 (3 mm, 36 degree groove, 1000 rpm,50kPa).

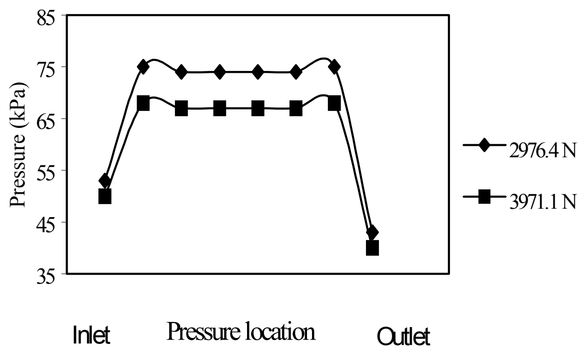

Figure 7. Measured axial pressure distribution (3 mm, 36 degree groove, 1000 rpm, 50kPa).

The non-metallic bearing was mounted in a steel sleeve with an interference fit and the sleeve-bearing assembly was fixed into the housing. Pressures were measured along the groove located in the loaded region of the bearing and around the circumference of the bearing half-way along its length for various operating conditions. There were 16 tapping points circumferentially and 7 axially. Special note was made of pressures near to the groove edges. Flexible tubes were fitted to each tapping point and taken to a manifold where the pressure was measured by a pressure transducer, one at a time. An air release valve was located near to the manifold.

The load was applied by a dead weight to the top of the bearing housing thereby ensuring that the minimum film thickness was located near to the top of the bearing. Only bearings with three equi-spaced axial grooves along the complete length of the bearing were tested. The angular extent of each groove was 36° or 18°, with the groove depth being maintained at 0.003m. The actual diametral clearance was measured to be 0.86×10^{-3}m.

The lubricant water, was fed from one end of the bearing through each of the three axial grooves and around the space between the shaft and the bearing bush. This pressure-fed situation, together with the rotation of the shaft, means that the flow conditions inside the bearing consisted of a combination of Couette flow (shaft velocity induced) and the axially fed Poiseuille flow. Published performance data on this arrangement was not available.

Static measurement capabilities include the flow rate, the inlet pressure and the outlet pressure to and from the bearings, rise in water temperature as it passes through the bearing, the shaft speed, the applied load and the power consumed by the three-phase electric motor.

The supply of lubricating water was maintained at around 7.4 l/min for different loads at different lubricant supply pressures. The flow rate was measured by transferring the water which flowed to the tank to a pail where it could be measured within one minute. Two different shaft speeds were established for each set of bearings. For shaft speeds of 1500 rpm and 1000 rpm, a constant lubricating supply pressure of 100 kPa, 75 kPa or 50 kPa was applied. Different loads were added to the load table for recording of the internal bearing pressures. Lead weights were used to apply the load. The 8kg mass of the load table was accounted for in the load increment.

The driving power of the three phase electric motor was determined for each load using the 'Clamp On Power Factor Tester' by recording the input voltage, the current from each phase and the power factor. The speed was measured with a hand held photosensitive tachometer for each load added to the load table. Also the inlet and outlet temperature of the water were recorded by connecting the thermocouples to an electronic analog thermometer. Bearing pressures at various measuring points were recorded.

Results and discussion

The pressure contours shown in figures 3 and 4 indicate that the maximum pressure in the clearance space of the bearing does not occur at the central plane but shifts closer to the outlet side of the bearing. This is because the lubricant is supplied axially. It is also observed from figures 6 and 7 that no flow takes place into the bearing at the inlet in the loaded region, because there is a positive pressure gradient. At the inlet, flow into the bearing takes place only in the unloaded region. At the outlet, flow takes place out of the bearing in the loaded region. The flow into and out of the bearing is maintained very much similar to that in a submerged bearing [5].

The test rig was used to measure the circumferential and axial pressure profiles around and along the bearing for various conditions of load, speed, geometry of groove and Poiseuille pressure supply.

Theoretical calculations using ESDU [1] in conjunction with ESDU [2] were performed to locate the position of the minimum film thickness through the attitude angle and eccentricity ratio. Inspection of figures 3 and 4 shows that at a point located inside the groove in the loaded section of the bearing, the pressure always remains constant at a value higher than the supply pressure. This has been validated by the experimental results as well.

Conclusions

1. The CFD results indicate that the maximum pressure zone in the bearing has moved towards the outlet. The pressure contours obtained, can be used to understand the flow characteristics of the bearing.
2. From the experimental results and the corresponding CFD analysis, it is observed that, the pressure along the axial groove located in the loaded area of the bearing and supplied with water at one end increased rapidly to a value which depended on the load applied to the bearing, remained constant along the length and then fell sharply to the outlet value. This is quite different to the hypothesis that there would be a linear change from the inlet pressure to the outlet value which was used in [4]. The implication here is that lubricant is squeezed out of both ends of the groove, that is, water does not enter this groove axially. Water clearly enters the bearing in the unloaded areas and is carried around the bearing by Couette action.

Acknowlegdements

The authors wish to acknowledge the experimental work carried out by a number of undergraduate students, namely, C S Tan, P Gleeson, Y S Tay, M Chiu and K Wang.

References

[1] ESDU International, Calculation Methods for Steadily Loaded Axial Groove Hydrodynamic Journal Bearings– Superlaminar Operation, London, *Engineering Sciences Data Item,* **85028,** 1984.

[2] ESDU International, Calculation Methods for Steadily Loaded Axial Groove Hydrodynamic Journal Bearings". London, *Engineering Sciences data Item,* **84031,** 1985.

[3] George, W., *Lubrication Fundamentals*, New York, Marcel Dekker Inc., 1980, 88-144.

[4] Hargreaves, D.J. and Elgezawy, A.S., Optimisation of Grooving Arrangements In water Lubricated Non-Metallic Journal Bearings, *Trans. IEAust*, **ME183**, 1993, 245-251.

[5] R. Pai and B. C. Majumdar,"Stability of submerged oil film journal bearings under dynamic load" WEAR, Vol 146, (1991) pp 125-135.

[6] Shelly, P. and Ettles, C., Solutions for the Load Capacity of Journal Bearings with Oil Grooves, Holes, Reliefs or Chamfers in Non-optimum Positions, *Proceeding of the Institution of Mechanical Engineers*, **C56/71**, 1971, 38-46.

[7] Sprengel, J. F. and Hargreaves, D. J., A test rig for the performance assessment of non-metallic water lubricated bearings, *International Tribology Conference, Brisbane, 3-5 December 1990*, Institution of Engineers, Australia National Conference Publication NCP 90/14.

[8] Vijayaraghavan, D. and Keith, T.G., Effect of Type and Location of Oil Groove on the Performance of Journal Bearings, *Tribology Trans*, **35** ,1992, 98-106.

.